Molecular, Enzymatic, and Regulatory Characterization of Rat Kidney Cytochromes P450 4A2 and 4A3[†]

Christian Helvig,[‡] Elizabeth Dishman,[‡] and Jorge H. Capdevila*[,‡,§]

Departments of Medicine and Biochemistry, Vanderbilt University Medical School, Nashville, Tennessee 37232

Received May 6, 1998; Revised Manuscript Received July 14, 1998

ABSTRACT: The cDNAs encoding cytochromes CYP 4A2 and 4A3 were cloned by RT-PCR amplification of male rat kidney and liver RNAs, respectively. Sequence analysis demonstrated that these cDNAs were nearly identical to the published sequences for CYPs 4A2 and 4A3. CYP 4A2 and 4A3 share extensive sequence homology that extends into their 3′- and 5′-untranslated segments (∼97% overall nucleotide identity). Analysis of cDNA and genomic DNA sequences shows that a sequence of 123 bp, recognized as an intron during the processing of CYP 4A2 transcripts, is conserved in the 4A3 mRNAs and that these otherwise highly homologous genes show different exon−intron distributions. The CYP 4A2 and 4A3 cDNAs were expressed in a baculovirus−insect cell expression system. Purified recombinant CYP 4A2 oxidized arachidonic acid to a mixture of 19- and 20-hydroxyeicosatetraenoic acids (20 and 80% of the total products, respectively). Reaction rates were maximal when CYP 4A2 was reconstituted in the presence of an equimolar concentration of cytochrome b_5 and a 10-fold molar excess of NADPH−cytochrome P450 reductase. Studies using microsomal fractions isolated from noninfected insect cells and from cells infected with CYP 4A3 recombinant baculoviruses showed (a) the presence of an endogenous lauric acid ω-hydroxylase and arachidonic acid epoxygenase in the noninfected cells, (b) the CYP 4A3-dependent oxidation of lauric acid to 11- and 12-hydroxylaurate (24 and 76% of the total products, respectively), and (c) the lack of arachidonic acid metabolism by microsomal recombinant CYP 4A3. Nucleic acid hybridization and immunoelectrophoresis studies demonstrated that (a) CYP 4A2 transcripts are abundantly expressed in the female kidney and that CYP 4A3 is expressed in female but not in male liver, (b) anti-CYP 4A2 immunoreactive material was detected only in the male kidney, (c) male and female livers or kidneys support only low levels of CYP 4A3 translation, and (d) excess dietary salt does not alter the kidney levels of mRNA transcripts encoding CYP 4A1, 4A2, or 4A3 or change the levels of microsomal anti-4A1 or -4A2 immunoreactive proteins. Finally, no significant differences were observed between Dahl salt resistant or Dahl salt sensitive rats in the levels and/or salt regulation of mRNA transcripts enecoding CYP 4A1, 4A2, or 4A3 or the in levels of the corresponding proteins.

Since the initial report of a role for microsomal cytochrome P450[1] in the NADPH-dependent metabolism of AA (*1*−*3*), results from several laboratories have demonstrated the tissue and isoform specific P450-dependent oxidation of AA via one or more of the following enzymatic pathways: (a) allylic oxidation generating six regioisomeric hydroxyeicosatetraenoic acids containing a cis,trans-conjugated dienol functionality (5-, 8-, 9-, 11-, 12-, and 15-HETE), (b) olefin epoxidation (epoxygenase reaction) affording four isomeric epoxyeicosatrienoic acids (5,6-, 8,9-, 11,12-, and 14,15-EET), and (c) hydroxylations at or near terminal sp^3 carbons (ω and $\omega - 1$ oxygenase reaction) yielding 16-, 17-, 18-, 19-, and 20-OH-AA (*5*−*9*, and references therein). The confirmation of stereoselective, in vivo formation of EETs by rat, rabbit, and human organs and of urinary excretion of EETs and 20-OH-AA (*4*−*8*, and references therein) established microsomal P450 as a formal member of the endogenous AA cascade and suggested a variety of novel functional roles for this important group of oxygenases (*4*−*8*). More recently, it has become apparent that the analysis of these functional roles will require (a) the identification and enzymatic characterization of the relevant P450 isoforms, (b) the analysis of their regulatory control by relevant hormones and/or functionally meaningful protocols of animal manipulation, and (c) the use of experimental models of genetically controlled dysfunction in which P450 isoform specific genotypes can be associated with specific functional alterations (*4*−*11*).

[†] This work was supported by U.S. Public Health Services Grant NIHDK 38226. N-Terminal amino acid microsequencing was carried out at the Vanderbilt Medical Center Protein Sequencing Core Facility, a Vanderbilt Cancer Center shared resource, supported by an NCI Center Grant (CA 68485).

* To whom correspondence should be addressed: Department of Medicine, Vanderbilt University Medical Center, Medical Center North S-3223, Nashville, TN 37232. Phone: (615) 322-4968.

[‡] Department of Medicine.

[§] Department of Biochemistry.

[1] Abbreviations: P450, cytochrome P450; AA, arachidonic acid; ORF, open reading frame; HETE, hydroxyeicosatetraenoic acid containing a cis,trans-conjugated dienol; EET, *cis*-epoxyeicosatrienoic acid; 19- and 20-OH-AA, 19- and 20-hydroxyeicosatetraenoic acid, respectively; DOCA, deoxycorticosterone acetate; DTT, dithiothreitol; SDS, sodium dodecyl sulfate; PAGE, polyacrylamide gel electrophoresis; HPLC, high-pressure liquid chromatography; RP, reversed phase; GC, gas−liquid chromatography; MS, mass spectral; NICI, negative ion, electron capture chemical ionization; PFB, pentafluorobenzyl; TMS, trimethyl ether silyl.

S0006-2960(98)01048-4 CCC: $15.00
Published on Web 08/19/1998

Male rat kidney microsomal fractions metabolized AA to 20-OH-AA, 19-OH-AA, and 11,12-EET as the major reaction products (*12*). Antibody inhibition and/or reconstitution experiments using tissue-purified P450s or recombinant proteins showed that (a) AA epoxidation was catalyzed, for the most part, by members of the CYP 2C gene family members and (b) CYP 2C23 was the major 2C epoxygenase isoform in the rat kidney (*5*−*7*, *12*, *13*). The role of CYP 4A isoforms in fatty acid ω and $\omega - 1$ oxidation is well established (*4*, *14*, and references therein, *15*). Thus, several tissue-purified and/or recombinant rat, rabbit, and human CYP 4A isoforms have been shown to catalyze fatty acid and prostanoid ω and $\omega - 1$ metabolism (*4*, *5*). The CYP 4A gene subfamily comprises a group of conserved, evolutionarily specialized fatty acid hydroxylases with little or no activity toward most other P450 substrates (*14*, *15*). While all characterized P450 4A proteins catalyze fatty acid ω or ω and $\omega - 1$ oxidation, at present, no 4A isoform has been shown to be selective only for $\omega - 1$ oxidation of fatty acids, including AA. Four 4A isoforms (4A1, 4A2, 4A3, and 4A8) have been cloned from rat tissues and sequenced (*4*, *16*, and references therein). The sequences and structures of the CYP 4A1 and 4A2 genes are published (*16*). Notwithstanding intensive cloning efforts, only the cDNA encoding CYP 4A1 has been expressed and shown to catalyze AA ω oxidation (*4*, *14*, *15*, *17*). A purified form of CYP 4A2 was shown to catalyze lauric and AA ω and $\omega - 1$ oxidation (*18*). Recently, a cDNA encoding CYP 4A2 was amplified by RT-PCR of rat kidney RNA and expressed in *Sf9* insect cells. Microsomal fractions isolated from these cells were shown to metabolize AA to a mixture of 20-OH-AA and 11,12-EET (*19*).

Several biological activities have been described for the products of the AA ω and $\omega - 1$ oxygenase (*4*−*9*). Some of these are species specific, vessel specific, and even systemic pressure-dependent (*4*−*9*). Furthermore, in some cases, the biological activities of these metabolites are mediated by prostaglandin H_2 synthase-catalyzed transformations (*4*−*9*). Some of the reported effects of the AA ω and $\omega - 1$ metabolites on ion transport may underline their vasoactive properties. Among these, 19(*S*)-OH-AA stimulated a partially purified renal cortical Na^+,K^+ ATPase (*7*, *9*). In rabbit mTALH cells, 20-OH-AA and the corresponding 1,20-dicarboxylic acid inhibited the Na^+,K^+,$2Cl^-$ cotransporter and a Na^+,K^+ ATPase (*7*, *9*). Both natriuretic and diuretic effects have been described for 20-OH-AA (*4*−*9*). Additionally, 20-OH-AA has been proposed as an endogenous inhibitor of Ca^{2+}-activated K^+ channels (*8*). The early proposal of a role for AA ω and $\omega - 1$ hydroxylation in the pathophysiology of experimental hypertension focused interest on the analysis of the role of CYP 4A isoforms in the metabolism and bioactivation of AA (*7*, *9*). Studies with the spontaneously hypertensive rat model (SHR/WKY model) indicated that, in these animals, the developmental phase of hypertension was linked to attendant increases in the activities of the kidney microsomal AA ω and $\omega - 1$ oxygenase (*7*, *9*). Importantly, hypertensive SHR animals could be made normotensive after induction of heme oxygenase by $SnCl_2$ administration, an effect attributed to an organ selective, $SnCl_2$-dependent depletion of the renal P450 AA ω and $\omega - 1$ oxygenase (*7*, *9*). The preferential expression of the CYP 4A2 gene in SHR hypertensive animals (*20*) and the cosegregation of the CYP 4A2 gene locus with the high-blood pressure phenotype in Dahl salt sensitive rats have been demonstrated (*21*). As part of our ongoing studies of the functional significance of the microsomal P450 AA monooxygenase, we report here the cloning of the cDNAs encoding the highly homologous CYPs 4A2 and 4A3, their structural and enzymatic characterization, their liver and kidney expression, and their regulation by dietary salt.

MATERIALS AND METHODS

Animals. Male or female Sprague-Dawley rats (280−320 g of body weight) and male Dahl salt resistant and Dahl salt sensitive rats (280−320 g of body weight) (outbred, Brookhaven National Laboratories, Long Island, NY) were purchased from Harlan Sprague Dawley, Inc. (Indianapolis, IN), and held at 22 °C with alternating 12 h cycles of light and dark. Animals were fed a standard rat chow containing 0.4% sodium or, for high salt treatments, a modified rat chow containing 8% NaCl (w/w) (Special Mix 5001-2, Ralston Purina Mills, St. Louis, MO). DOCA (5 mg/kg of body weight), in corn oil, was administered for 2 weeks by single, daily, intraperitoneal injections (*10*, *12*, *22*). The mean arterial blood pressures (MAPs) of SHR and Dahl rats were determined, at 30 °C, by the tail cuff method using a blood pressure analyzer instrument (model 178, IITC, Life Science USA, Woodland Hills, CA) and the manufacturer's instructions.

Cloning and Characterization of the cDNAs Encoding CYPs 4A2 and 4A3. Total RNA (5 μg), isolated from male kidney or liver DNA, was reverse transcribed utilizing a 16-mer oligo-dT primer (Perkin-Elmer, Norwalk, CT) and Superscript polymerase (Gibco BRL, Gaithersburg, MD) (2.5 μM and 10 000 units/mL final concentrations, respectively). After 1 h at 40 °C, the reactions were terminated by heating (100 °C, 2 min) and the products utilized as PCR templates. PCR amplifications were carried out in 10 mM Tris-HCl (pH 8.3), 50 mM KCl, 1.5 mM $MgCl_2$, and 0.5 mM dNTPs, containing 50 units/mL of ampliTaq DNA polymerase (Perkin-Elmer) and each of the following primers at 0.15 μM: a 20-mer antisense oligonucleotide common for CYP 4A2 and 4A3 (5′-GGATTTATTTACAGTTTGGC-3′) and either a 20-mer (5′-AGACCCTAGTGATCCAGAAG-3′) or a 22-mer (5′-ATTAACCATGGGTTTCTCTGTA-3′) sense primers, specific for CYPs 4A2 and 4A3, respectively (*16*). Gel-purified PCR products were ligated into the pCR2.1 vector (Invitrogen, La Jolla, CA). Insert-containing plasmids (2 and 2.1 kb for CYPs 4A2 and 4A3, respectively) were replicated in *Escherichia coli* (One shot cells, Invitrogen) and purified using a QIAprep Spin Maxiprep Kit (Qiagen Inc., Chatsworth, CA) following the manufacturer's instructions. After restriction endonuclease analysis, the CYP 4A2 and 4A3 cDNA inserts were individually sequenced by the dideoxy chain termination method (*23*) using sequenase (U.S. Biochemicals, Cleveland, OH). Approximately 30 oligonucleotides/insert (15−20-mer each) spanning the length of each cDNA were utilized as primers for the sense and antisense cDNA strands. Ambiguities were resolved by sequence analysis of clones derived from different RT-PCR products and/or PCR amplification of genomic DNA. Nucleotide sequences were analyzed utilizing DNASIS Sequence Analysis Software (Hitachi Software, San Fran-

cisco, CA) and the Nucleotide Data Base (NCBI, Washington, DC).

To construct a P450 chimera containing the first 545 nucleotides of the cDNA encoding CYP 4A3 (from the ATG initiation codon) and nucleotides 536−1515 from the cDNA encoding CYP 4A2 (from the ATG initiation codon), a CYP 4A3 *Nco*I−*Bgl*II fragment was ligated to a CYP 4A2 *Bgl*II−*Sca*I fragment. The chimeric cDNA was cloned into the pBlue-Bac vector and, after confirming sequence integrity, expressed in a baculovirus−*Sf*9 cell system as below.

Nucleic Acid Blot Hybridization. Samples of total RNA were isolated from the livers and kidneys of control or salt- or DOCA-treated animals, denatured, and electrophoresed as described (*12*, *42*). After capillary-pressure transfer to nitrocellulose membranes, the blots were hybridized to the following CYP 4A nucleotide probes: (a) a CYP 4A1 specific fragment (695 bp) encoding a segment of the cDNA 3′-untranslated sequence and generated by *Sac*I−*Eco*RI digestion of the CYP 4A1 cDNA (*25*), (b) a CYP 4A2 and 4A3 specific probe (542 bp) containing a portion of the cDNA 3′-untranslated sequences and obtained after *Bam*HI−*Xho*I digestion of the CYP 4A2 cDNA, (c) a CYP 4A2 specific probe (123 bp) generated by PCR amplification of the corresponding cDNA using sequence specific 22-mer primers (sense, 5′-TGGGATCCACCTGCGTCTCAAG-3′; and antisense, 5′-GAGGTGAAACCAGATGGGAAAT-3′) (*26*), and (d) a CYP 4A3 specific probe (121 bp) generated by PCR amplification of the corresponding cDNA using sequence specific 20-mer primers (sense, 5′-GTCTGCTGC-CTGCAATACCT-3′; and antisense, 5′-CTACAGAAAT-GAGGGCAAAA-3′) (*27*). The blots were hybridized with ^{32}P-labeled probes for 14 h at 42 °C and in Hybrisol I (Oncor Inc., Gaithersburg, MD). Double-stranded probes were labeled by nick translation using *E. coli* polymerase I and [α-^{32}P]ATP. After exposure, the blots were stripped at 90 °C and rehybridized to a cDNA probe encoding rat liver β-actin.

For the selective RT-PCR amplification of CYP 4A2 or 4A3 fragments, the following isoform specific primers were utilized: (a) for 4A2, 18 bp, 5′-CAAAGCCTTATCAATCCC-3′, between nucleotides 331 and 350, from the initiation ATG codon; and (b) for 4A3, 20 bp, 5′-GGCTTCTGGAATT-TATCAAT-3′, between nucleotides 335 and 356, from the initiation ATG codon. RT-PCR amplification was done with these oligonucleotides, as sense primers, and a 20 bp antisense primer common to CYPs 4A2 and 4A3 (5′-GGATTTATTTACAGTTTGGC-3′, between nucleotides 1968 and 1989, from the initiation ATG codon in CYP 4A2).

Heterologous Expression and Purification of Recombinant CYP 4A2. High-yield expression of the cloned cDNAs was achieved with a MAXBAC Baculovirus Expression System (Invitrogen) following the manufacturer's instructions. Briefly, the 4A2 and 4A3 cDNA inserts were released from the pCR2.1 plasmid by either *Nco*I and *Sca*I digestion (1922 bp, CYP 4A2) or *Nco*I and *Bsa*BI digestion (1621 bp, CYP 4A3) and individually subcloned into the *Nco*I and a blunted *Hin*dIII site of the pBlueBac4 vector. Cultured *Sf*9 cells were transfected with a mixture of the CYP 4A2- or 4A3-containing vector and the wild type baculovirus in cationic liposomes. Recombinant viruses were isolated and purified, and the presence of a 4A2 or 4A3 insert was corroborated by PCR. Cultured *Sf*9 cells were infected with either the CYP 4A2 or 4A3 recombinant baculovirus at a multiplicity of 10 viruses/cell. Hemin (10 μM final concentration) was added after 24 h at 27 °C, and the cells were collected after an incubation for an additional 24 h at 27 °C.

For purification of recombinant CYP 4A2, cells were lysed in 0.1 M sodium phosphate buffer (pH 7.4) containing 20% (v/v) glycerol, 0.1 mM EDTA, 0.1 mM DTT, and 1% (w/v) sodium cholate. After 1 h at 4 °C, insoluble proteins were removed by centrifugation (1 h at 140000*g*), the P450 and sodium cholate concentrations of the high-speed supernatant were adjusted to 1 μM and 0.4%, respectively, and the resulting solution was immediately loaded onto a octyl-Sepharose 4B (Pharmacia Biotech AB, Uppsala, Sweden) column (5 cm × 10 cm). Extensive column washing was followed by elution of bound CYP 4A2 in the presence of 0.4% (v/v) Emulgen 911 (Kao Chemical Co., Tokyo, Japan) as described in Results and Discussion. After dialysis versus 20 mM Tris-HCl containing 20% (v/v) glycerol, 0.1% (w/v) sodium cholate, and 0.1 mM DTT (buffer A) (16 h, 100 volumes), the CYP 4A2 sample was loaded onto a hydroxylapatite (Bio-Rad Laboratories, Richmond, CA) column (2 cm × 12 cm) equilibrated with buffer A containing 0.4% (v/v) Emulgen 911. The column was washed with 10 volumes of the equilibrating buffer, and the bound P450 4A2 was then eluted in the presence of 0.3 M sodium phosphate (pH 7.4) in buffer A. Overnight dialysis [versus 100 volumes of buffer A containing 0.1 mM EDTA and 0.2% (v/v) Emulgen 911, instead of sodium cholate (buffer B)] was followed by chromatography on a Bio-gel A DEAE (Bio-Rad Laboratories) column (1 cm × 10 cm) equilibrated with buffer B. Approximately 80% of the P450 loaded onto this column eluted during loading and washing. A second fraction, containing less than 2% of the material initially applied, was eluted when the NaCl concentration in buffer B was raised linearly from 0 to 0.3 M. The fraction not retained by the Bio-gel A DEAE column, containing recombinant CYP 4A2, was dialyzed overnight versus 100 volumes of buffer A. Emulgen 911 was removed by hydroxylapatite chromatography as in ref *28*, and after dialysis (16 h, 100 volumes, buffer A), the resulting sample was utilized for analysis and characterization.

Microsomal fractions were isolated from control and insect cells infected with the CYP 4A3 or CYP 4A2 recombinant baculovirus by differential centrifugation methods. Briefly, cells were collected and washed twice by centrifugation (4000*g* for 5 min each). Cell pellets were suspended in 10 mM Tris-HCl buffer (pH 7.5) containing 0.25 M sucrose, 1 mM EDTA, 0.5 mM phenylmethanesulfonyl fluoride, 0.1 μg/mL leupeptin, and 0.04 unit/mL aprotinin, sonicated twice (50% of full power) (Ultrasonic 4710, Cole Parmer Ins. Co., Chicago, IL), and centrifuged at 12000*g* for 15 min, and the supernatants were centrifuged at 105000*g* for 60 min. Prior to being utilized, microsomal fractions were suspended in 10 mM Tris-HCl buffer (pH 7.5) containing 0.25 M sucrose.

Enzymatic Activities and Product Characterization. Purified recombinant CYP 4A2 (50−250 pmol) was sequentially mixed with a solution of dilauroylphosphatidylcholine (1 mg/mL, 10−100 μL), NADPH−P450 reductase (20 μM, 2−30 μL, to obtain P450/NADPH−P450 reductase molar ratios between 1/1 and 1/20), and, when added, cytochrome b_5 (5 μM, 2−10 μL, to obtain P450/cytochrome b_5 molar ratios between 2/1 and 1/5). After 10 min at room temperature,

the enzyme mixture was diluted 10-fold by the addition of 50 mM Tris-HCl buffer (pH 7.5) containing 10% glycerol, 0.15 M KCl, 10 mM $MgCl_2$, 8 mM sodium isocitrate, and isocitrate dehydrogenase (0.5 IU/mL) and the mixture preincubated for 1 min at 35 °C prior to the addition of either [1-^{14}C]AA (10−50 μCi/μmol, 50−100 μM final concentration) or [1-^{14}C]LA (2−10 μCi/μmol, 50−70 μM final concentration). Microsomal fractions, isolated from control or recombinant baculovirus-infected cells, were suspended (1.0−2.0 mg of protein/mL) in 50 mM Tris-HCl buffer (pH 7.5) containing 0.15 M KCl, 10 mM $MgCl_2$, 8 mM sodium isocitrate, and isocitrate dehydrogenase (0.5 IU/mL), and the mixture was incubated for 10 min (23 °C) in the presence of purified rat liver NADPH−P450 reductase (0.1 μM final concentration). After 1 min at 35 °C, the radiolabeled fatty acids were added to a final concentration of 50−100 μM. Reactions were initiated by the addition of NADPH (1 mM final concentration) and continued at 35 °C while the solutions were mixed constantly. Aliquots of the reaction mixture were withdrawn at different time points and the organic soluble products extracted into acidified ethyl ether, resolved by RP-HPLC (*29*), and quantified by on-line liquid scintillation using a Flo-one β counter (Radiomatic Instruments, Tampa, FL).

Synthetic 20- and 19-OH-AA were resolved by normal phase HPLC on a 5 μm Dynamax Microsorb Silica column (4.6 mm × 250 mm, Rainin Instruments Co., Woburn, MA) and a solvent mixture of 1% 2-propanol, 0.1% HOAc, and 98.9% hexane at 3 mL/min ($t_R \sim$ 14.1 and 20.5 min for 19- and 20-OH-AA, respectively). 11,12- and 14,15-EET were resolved and characterized as described (*30*). 11- and 12-dodecanoic acids (11- and 12-OH-LA, respectively) were resolved by reversed phase HPLC on a 5 μm Dynamax Microsorb C_{18} column (4.6 cm × 250 cm, Rainin Instruments Co.) using a solvent mixture composed of 29.5% CH_3CN, 69.5% H_2O, and 0.1% HOAc which was isocratic for 5 min, followed by a linear gradient to 59.5% CH_3CN, 39.5% H_2O, and 0.1% HOAc over 30 min ($t_R \sim$ 19.6 and 21.9 min for 11- and 12-OH-LA, respectively). PFB esters were prepared by reaction with pentafluorobenzyl bromine (*30*). TMS ethers were prepared by reaction with bis(trimethylsilyl)-trifluoroacetamide (Supelco Inc., Bellefonte, PA) in pyridine (*30*). Catalytic hydrogenations were performed as in ref *30*. NICI−GC−MS analyses were performed as reported previously (*30*).

Other Methods. Polyclonal antibodies against purified recombinant CYP 4A2 were raised in female White New Zealand rabbits as described previously (*12*). The anti-4A2 IgG was purified by affinity chromatography on a Protein G Superose HR 10/2 column (Pharmacia Biotech AB). After $(NH_4)_2SO_4$ precipitation and dialysis against 20 volumes of 20 mM sodium phosphate buffer (pH 7.0) (*12*), samples of anti-4A2 rabbit IgG were loaded (at 1 mL/min) onto the affinity column and the column then was washed for 10 min with equilibration buffer [20 mM sodium phosphate buffer (pH 7.0)]. Anti-4A2 antibodies were eluted with a linear buffer gradient from initially 100% equilibration buffer to 100% 100 mM glycine (pH 2.7) over 20 min at a flow rate of 1 mL/min. Purified goat anti-P450 4A1 IgG was a gift from G. Gibson (Department of Biochemistry, University of Surrey, Gilford, Surrey, England). Cytochrome b_5 and rat liver NADPH−P450 reductase were purified to electrophoretic homogeneity (*28*). Discontinuous SDS−PAGE (10% w/v acrylamide, 100 mm × 60 mm × 1 mm slabs) were like those in ref *28*. Resolved proteins were transferred electrophoretically onto PVDF membranes and immunoblotted exactly as described previously (*12*). Antigen−antibody reactions were detected using a SuperSignal Substrate Western Blotting kit (Pierce, Rockford, IL) and the manufacturer's instructions. Spectral studies were carried out, at room temperature, in an Aminco DW2 spectrophotometer. Cytochrome P450 concentrations were determined as in ref *31*. Protein concentrations were determined using the Bio-Rad Protein Assay reagent (Bio-Rad Laboratories). N-Terminal amino acid analyses were carried out in an Applied Biosystems 470A instrument (Applied Biosystems, Foster City, CA). Purified P450s were submitted to SDS−PAGE in 200 mm × 120 mm × 1.5 mm slabs using a 7 to 12% (w/v) polyacrylamide gradient as the separating gel. Proteins were electroblotted onto poly(vinylidene difluoride) membranes, stained with Coomassie brilliant blue R-250 (Bio-Rad Laboratories), and sequenced in the membrane after removal of the protein stain (*32*). Cycle yields were calculated by comparisons with internal standards.

RESULTS AND DISCUSSION

cDNA Cloning and Characterization. Amino acid sequence comparisons indicated that the rat 4A isoforms could be divided into two subgroups that share a ≥71% overall homology (*25*−*27*, *33*). One group is composed of CYPs 4A1 and 4A8 (with a 76% amino acid sequence identity among them), and the other is composed of the highly homologous CYPs 4A2 and 4A3 (*25*−*27*, *33*). CYP 4A1 was the first rat CYP 4A isoform cloned and characterized (*17*, *25*). Heterologous expression and characterization showed that recombinant CYP 4A1 metabolized AA selectively at its ω-carbon (*17*, *29*). The extensive sequence homology between CYPs 4A2 and 4A3 (≥96.4% identity at the amino acid or nucleotide level) (*26*, *27*) has complicated the analysis of their organ and/or gender specific expression and/or distribution. On the other hand, CYPs 4A2 and 4A3 show a more limited sequence homology with respect to CYPs 4A1 (≤72%) and 4A8 (≤71%) (*17*, *25*−*27*, *33*). Published nucleic acid hybridization studies showed that while CYPs 4A1 and 4A3 were preferentially expressed in livers of male Sprague-Dawley rats, CYPs 4A2 and 4A8 predominated in the kidney (*17*, *25*−*27*, *33*, *34*). Therefore, we isolated total RNA from the livers and kidneys of male rats and utilized them for RT-PCR amplification and cloning of the cDNAs encoding kidney CYP 4A2 and liver CYP 4A3.

Sequence analysis demonstrated that the 4A2 cDNA clone contained a 2027 bp insert with an ORF, encoding a protein of 504 amino acids, flanked by initiation and termination codons between nucleotides 29 and 1541, respectively. Compared to the published CYP 4A2 sequence (*26*), the clone contained a 123 bp deletion (between nucleotides 1542 and 1665, from the ATG initiation codon) (Figure 2) near the middle of the proposed exon 12 (*26*) (Figure 2). Genomic analysis showed that this deletion, common to all 4A2 clones that were analyzed, arose from mRNA processing and not genetic heterogeneity. We concluded that this 123 bp segment corresponded to a CYP 4A2 intron and that, as with the CYP 4A1 gene (*25*), the CYP 4A2 gene contains

```
          10        20        30        40        50        60
4A2  MGFSVFSPTRSLDGVSGFFKGAFLLSLFLVLFKAVQFYLRRQWLLKALEKFPSTPSHWLW
4A3  ......T...........Q.....................................
          10        20        30        40        50        60

          70        80        90       100       110
4A2  GHNLKDREFQQVLTWVEKFPGACLQWLSGSTARVLLYDPDYVKVVLGRSDPK---PYQSL
4A3  ..D.........................KT.................ASGI..F.
          70        80        90       100       110       120

     120       130       140       150       160       170
4A2  APWIGYGLLLLNGKKWFQHRRMLTPAFHYDILKPYVKIMADSVSIMLDKWEKLDDQDHPL
4A3  ............................G.............................
          130       140       150       160       170       180

     180       190       200       210       220       230
4A2  EIFHYVSLMTLDTVMKCAFSHQGSVQLDVNSRSYTKAVEDLNNLIFFRVRSAFYGNSIIY
4A3  ........................................T...............
          190       200       210       220       230       240

     240       250       260       270       280       290
4A2  NMSSDGRLSRRACQIAHEHTDGVIKTRKAQLQNEEELQKARKKRHLDFLDILLFAKMEDG
4A3  ........................M.................................
          250       260       270       280       290       300

     300       310       320       330       340       350
4A2  KSLSDEDLRAEVDTFMFEGHDTTASGISWVFYALATHPEHQERCREEVQSILGDGTSVTW
4A3  ............................................................
          310       320       330       340       350       360

     360       370       380       390       400       410
4A2  DHLDQMPYTTMCIKEALRLYSPVPSVSRELSSPVTFPDGRSIPKGIRVTILIYGLHHNPS
4A3  .....IS.............P.........................TT............
          370       380       390       400       410       420

     420       430       440       450       460       470
4A2  YWPNPKVFDPSRFSPDSPRHSHAYLPFSGGARNCIGKQFAMNELKVAVALTLLRFELLPD
4A3  ............................................................
          430       440       450       460       470       480

     480       490       500
4A2  PTRIPVPMPRLVLKSKNGIHLRLKKLR
4A3  ........A.................
          490       500
```

FIGURE 1: Comparison of the translated amino acid sequences for CYPs 4A2 and 4A3. The amino acid sequences shown were translated from the nucleotide sequences of the cloned kidney 4A2 and liver 4A3 cDNAs. Residue identity is indicated by dots. Amino acid differences are indicated in the primary structure of CYP 4A3.

13 exons, instead of the 12 previously described (*26*) (Figure 2). Consistent with this interpretation, splice donor−acceptor consensus sequences are found in the CYP 4A2 gene between exons 12 and 13 and the intervening 123 bp intron (Figure 2). Removal of the 123 bp intronic segment from the published sequence of the CYP 4A2 cDNA (*26*) resulted in a cDNA with sequence 99.7% identical to that of our clone. A total of six base substitutions were observed at nucleotides 87 (C for A), 1603 (C for T), 1607 (G for T), 1617 (G for C), 1805 (A for T), and 1864 (G for A) (*26*). The deduced amino acid sequence for CYP 4A2 contained a putative heme-binding peptide FSGGARNCIGKQFAM with the underlined conserved residues and the invariable cysteine at position 451 (Figure 1). Of the replacements described, only the C for A substitution (at nucleotide 87) yielded a translated protein with a nonconserved replacement of a basic glutamine for a neutral lysine (at residue 20) (Figure 1) (*26*). Since (a) this type of amino acid replacement could alter catalytic activity and (b) CYP 4A2 has been implicated in the pathophysiology of genetically controlled experimental hypertension (*7*, *9*, *21*), we determined the genomic basis of this nucleotide replacement. Samples of genomic DNA and total RNA were isolated from the livers of individual rats, and a 0.4 kb fragment, encoding exon 1 of CYP 4A2, was amplified by either PCR (genomic DNA) or RT-PCR (total RNA). Cloning and sequence analysis demonstrated that both the genomic and cDNA clones contained the same nucleotide substitution. Furthermore, a similar analysis performed using liver genomic DNA from Dahl salt sensitive, Dahl salt resistant, and SHR rats demonstrated that, for all DNAs, the sequences were identical to that of the cDNA cloned from Sprague-Dawley rats.

Sequence analysis of the liver 4A3 cDNA clone demonstrated that it contained a 2140 bp insert with sequence that

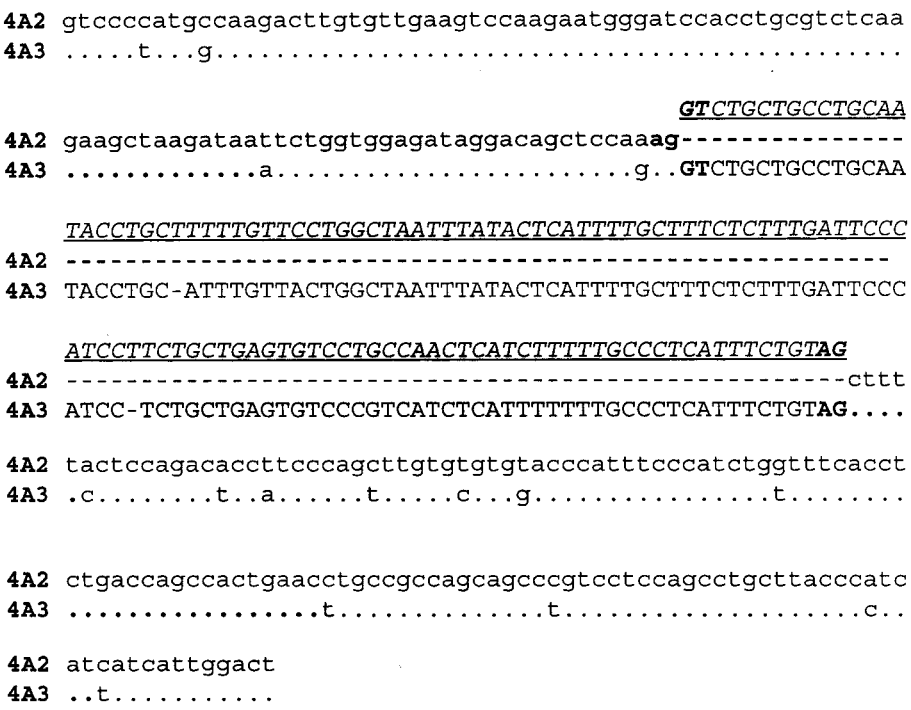

FIGURE 2: Nucleotide sequence alignments of the CYP 4A2 gene region encoding a segment of exons 12 and 13 and the intervening intron and a segment of exon 12 in CYP 4A3. The cDNA sequence alignments were initiated at residue 1446 (4A2) and 1455 (4A3) from the corresponding ATG initiation codons. A 123 bp gap (underlined), corresponding to the intron separating exons 12 and 13 in the CYP 4A2 gene, was introduced to maximize cDNA sequence homology. Putative splice recognition sequences are bold.

is 99.8% identical to that of a previously cloned cDNA (*27*). Our clone contained a total of three base substitutions (G for A, T for C, and T for C at nucleotides 491, 945, and 1099, respectively, from the initiation ATG codon), leading to two conserved (nucleotides 491 and 1099) and one silent (nucleotide 945) amino acid replacement (*27*). The cDNAs encoding CYPs 4A2 and 4A3 share extensive sequence homology that extents into their 5′- and 3′-untranslated areas (96.4% sequence identity, after the introduction of a 123 bp gap) (Figure 2). The 4A3 cDNA contained a nucleotide segment highly homologous to the putative 123 bp intron separating exons 12 and 13 in CYP 4A2 (*26*) (Figure 2). The size and the relative position of this segment (121 bp, between nucleotides 1552 and 1674, from the initiation ATG codon) indicated that it originated from differences in the splicing and/or processing of 4A2 and 4A3 transcripts. The molecular basis for these differences in the RNA processing mechanism for these two otherwise highly homologous genes remains to be elucidated. It is interesting that an alignment of cDNAs encoding several 4A P450 isoforms, including human 4A11, murine 4A10, rabbit 4A4, 4A5, 4A6, and 4A7, and rat 4A1, 4A2, 4A3, and 4A8, shows a 9 bp deletion in the ORF of rat CYP 4A2, unique to this isoform, and located in a cDNA region highly conserved among all 4A isoforms (approximately 140 bp, from nucleotide 62 to 200) (*16*). This area of high amino acid sequence conservation among 4A isoforms corresponds to the first substrate recognition domain initially described for 2C isoforms by Gotoh (*30*).

Finally, the CYP 4A3 cDNA contained an ORF, encoding a protein of 507 amino acids, flanked by initiation and termination codons at nucleotides 13 and 1534, respectively (Figure 1). The deduced amino acid sequence for CYP 4A3 contained a putative heme-binding peptide, FSGGARNCIGKQFAM, identical to that in CYP 4A2, with the underlined conserved residues and the invariable cysteine at position 454 (Figure 1). A comparison of the amino acid sequences of the translated 4A2 and 4A3 polypeptides shows that, with the exception of an extra A-S-G oligopeptide in CYP 4A3 (between amino acids 112 and 116), the encoded proteins are remarkably homologous (Figure 1). A total of 12 conserved and four nonconserved amino acid differences are more or less evenly distributed along the entire length of the encoded proteins (Figure 1). Of these differences, likely to affect isoform catalytic activity are (a) the presence (CYP 4A3) or absence (CYP 4A2) of the above-mentioned A-S-G oligopeptide and (b) the nonconserved amino acid sequence differences immediately after the A-S-G oligopeptide (112-PYQS-117 and 115-IYQF-120) for CYP 4A2 and 4A3, respectively (Figure 1).

Heterologous Expression and Enzymatic Characterization. The CYP 4A2 and 4A3 cDNA inserts were cloned into the pBlueBac4 vector and expressed using *Sf9* insect cells. Levels of 70−80 nmol of P450/L of culture were regularly observed with CYP 4A2. However, under identical conditions, we were unable to achieve spectrally detectable levels of CYP 4A3 expression. Recombinant CYP 4A2 was purified as described in Materials and Methods (*28*). More than 95% of the CYP 4A2 present in the *Sf9* cell lysate and loaded into the ω-aminooctyl-Sepharose 4B column (*28*) was retained by the resin, while most of the insect cell proteins eluted during sample loading and elution (Table 1 and Figure 3) (*28*). Of the P450 that was loaded, approximately 70% was then eluted in the presence of Emulgen 911. As shown in Figure 3 and Table 1, this simple, high-yield chromatographic step afforded a significantly purified hemoprotein (Table 1). After chromatography on hydroxylapatite and dialysis, the sample was resolved into two P450-containing fractions by chromatography in Bio-gel A DEAE (Bio-Rad

Table 1: Purification of Recombinant CYP 4A2 from Insect Cell Lysates

step	protein (mg)	P450 (nmol)	yield (%)	specific content (nmol/mg)
cell lysate	458	58.5	100	0.1
ω-aminooctyl-Sepharose 4B	83	40.4	69	0.5
hydroxylapatite	20	21.7	37	1.1
DEAE (not retained)	2	9.5	14	5.0
DEAE (0.2 M NaCl)	6	0.7	1	0.1

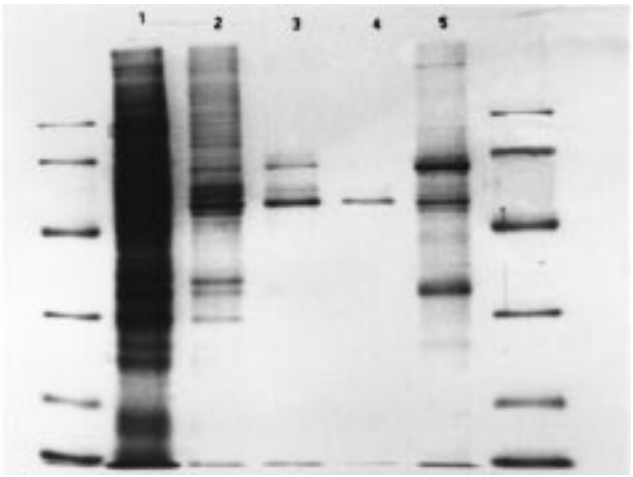

FIGURE 3: SDS−PAGE of fractions isolated during the purification of recombinant CYP 4A2 from insect cell lysates. Fractions (0.2−1.0 pmol of P450 each) were submitted to discontinuous SDS−PAGE in 10% acrylamide slab gels (1 mm thickness). After a 2−3 h staining in fresh 10% (w/v) Coomassie brilliant blue R-250 dye, the gels were destained by repeated washing in a solution containing 10% (v/v) CH_3OH and 0.7% (v/v) HOAc: lane 1, cell lysate; lane 2, ω-aminooctyl-Sepharose fraction; lane 3, hydroxylapatite fraction; lane 4, fraction not retained by the DEAE column; and lane 5, fraction eluted from the DEAE column in the presence of 0.2 M NaCl. Molecular weight standards were as follows: phosphorylase B, 97 400; serum albumin, 66 000; ovalbumin, 45 000; carbonic anhydrase, 31 000; and trypsin inhibitor, 21 500.

Laboratories). The first, containing recombinant CYP 4A2, was not retained by the column and accounted for ≥40% of the sample's hemoprotein. The second, containing a yet to be characterized P450, eluted at approximately 0.15−0.20 M NaCl and accounted for ≤1% of the P450 loaded into the column (Table 1 and Figure 3). Dialysis followed by removal of excess Emulgen 911 afforded (in 14% overall yield) a recombinant CYP 4A2 with a specific content of 5 nmol/mg of protein that, after SDS−PAGE, yielded a single predominant band with an approximate molecular weight (MW) of 58 000 (Table 1 and Figure 3). On the basis of this and the presence of a single amino-terminal sequence, we conclude that the sample contains highly purified CYP 4A2 and significant amounts of CYP 4A2 apoprotein (*28*, *36*).

A recently expressed CYP 4A2, cloned by RT-PCR of rat kidney RNA, was characterized by immunoelectrophoresis as a 52 000 MW protein (*19*), a size incompatible with the ORF predicted from the published cDNA sequence (*26*). N-Terminal amino acid analysis of the purified protein demonstrated that, with the exception of a missing amino-terminal methionine, the sequence of the first 13 amino acids of the recombinant protein was identical to that predicted from the proposed cDNA ORF (not shown). These results,

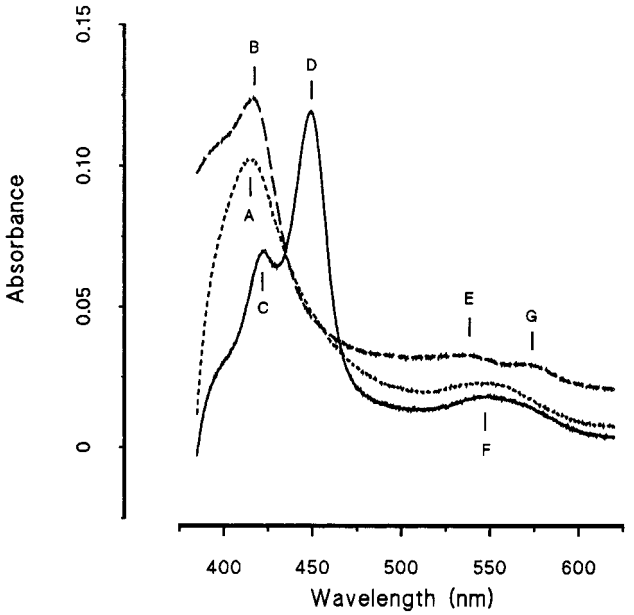

FIGURE 4: Spectral properties of purified recombinant CYP 4A2. Spectra were recorded, at 22 °C, with a solution of CPY 4A2 (1.1−1.3 μM final concentration) in 25 mM Tris-HCl buffer (pH 7.5) containing 20% glycerol and in an Aminco DW-2 spectrophotometer in the split beam mode. After the hemoprotein oxidized spectra were recorded (− − −), a few milligrams of $Na_2S_2O_4$ was added to the contents of the sample cuvette and the spectra of reduced CYP 4A2 were then recorded (- - -). The CO-bound spectra of reduced CYP 4A2 was recorded after the sequential addition of $Na_2S_2O_4$ and CO (−). Absorption maxima were at (A) 418, (B) 415, (C) 422, (D) 449, (E) 537, (F) 549, and (G) 571 nm.

as well as the results of the SDS−PAGE shown in Figure 3, confirmed the proposed ORF and 57 966 as the molecular weight for this hemoprotein.

The absolute spectrum of oxidized recombinant CYP 4A2 showed Soret, α, and β bands at 418, 571, and 537 nm, respectively (Figure 4). The presence of a shoulder at around 392 nm indicated that the recombinant protein was isolated in a mixed spin state (Figure 4). Reduction with sodium dithionite resulted in the attenuation and displacement of Soret band maxima to 415 nm, and the replacement of the α and β bands for a broad absorption band centered at around 546 nm (Figure 4). The addition of CO to a solution of reduced CYP 4A2 led to the rapid development of a strong absorption band with a maximum at 449 nm and shoulders at 422 and 549 nm (Figure 4), indicative of the formation of the CO-bound complex of reduced CYP 4A2. In experiments in which CO was added to the cuvette prior to reduction, it was observed that CYP 4A2 reduction was rapid and completed within the first few seconds of dithionite addition.

Among mammalian P450s, the members of the 4A gene subfamily are characterized by their high degree of structural and functional homology (*16*, *25*−*27*, *33*). Thus, in contrast to most P450s, 4A isoforms are highly selective with respect to fatty acid and prostanoid hydroxylation (*4*, *6*, *14*−*16*). A role for these proteins in endogenous fatty acid and prostanoid hydroxylation has been documented (*14*−*16*). Incubation of AA with a reconstituted system containing recombinant CYP 4A2, purified rat liver NADPH−cytochrome P450 reductase, and cytochrome b_5 (0.1, 5, and 0.01 μM final concentrations, respectively) resulted in the time-

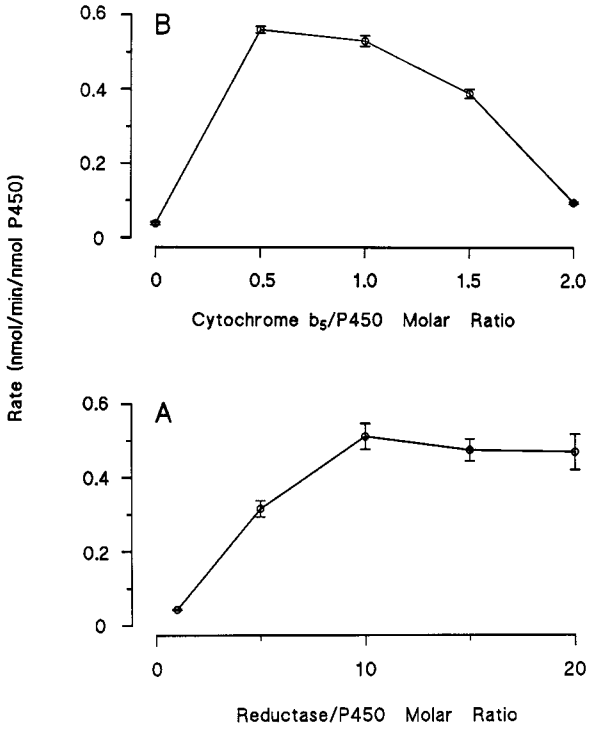

FIGURE 5: Cytochrome P450 reductase and cytochrome b_5 requirements of the AA monooxygenase reaction catalyzed by recombinant CYP 4A2. Recombinant CYP 4A2 (0.1 μM final concentration) was incubated with the concentrations of NADPH, [1-^{14}C]arachidonic acid, and dilauroylphosphatidylcholine described in the legend of Figure 6 and either in the presence of increasing concentrations of cytochrome P450 reductase (A) or, alternatively, in the presence of increasing concentrations of cytochrome b_5 and a 15-fold molar excess of cytochrome P450 reductase (B). After 15 min at 35 °C, the reaction products were extracted, resolved by RP-HPLC, and quantified by on-line liquid scintillation as described in Materials and Methods.

dependent formation of two metabolites with RP-HPLC retention times similar to those of authentic 19- and 20-OH-AA (not shown). Catalytic turnover was highly dependent on the concentrations of CYP 4A2, NADPH−cytochrome P450 reductase, and cytochrome b_5, as well as on the presence of dilauroylphosphatidylcholine (between 50 and 100 μg/mL) and KCl (150 mM). As shown in Figure 5A, enzyme activity increased almost linearly with increasing reductase concentrations, reaching a maximum at a ratio of approximately 10 mol of reductase per mole of CYP 4A2 (*28*). No significant differences in metabolite profiles were observed when the NADPH−cytochrome P450 reductase/P450 4A2 molar ratio was varied between 1 and 20 (*19*). As previously demonstrated for CYP 4A isoforms (*14*−*16*), the rate of AA oxidation by CYP 4A2 was significantly enhanced in the presence of cytochrome b_5 (Figure 5B). Optimal activity was obtained when the cytochrome b_5/P450 4A2 molar ratios were maintained between 0.5 and 1.0 (Figure 5B). Changes in the concentration of the added cytochrome b_5 had no effect in the chemistry of the reaction products. Under optimal conditions (1 mM NADPH, 50 μg/mL dilauroylphosphatidylcholine, 75−100 μM AA, and a NADPH−cytochrome P450 reductase/P450 4A2/cytochrome b_5 molar ratio of 10/1/1), AA was oxidized at a rate of 0.51 $\pm$ 0.03 nmol min^{-1} nmol^{-1} of P450 at 35 °C. Under similar conditions, the enzyme oxidized lauric acid to a mixture of 12- and 11-hydroxylauric acid at a rate of 10 nmol min^{-1} nmol^{-1} of P450.

For product structural analysis, the enzyme was incubated with [1-^{14}C]AA (75 μM, 15 μCi/μmol, approximately 24 at. % enrichment in ^{14}C) (*29*), and after organic solvent extraction and RP-HPLC product resolution, 1-^{14}C-labeled metabolites eluting form the RP-HPLC column between 14 and 16 min were collected batchwise and resolved by normal phase HPLC into two fractions that coeluted with samples of authentic 19- and 20-OH-AA. Fraction A was identified as 19-OH-AA on the basis of the following results: (1) coelution in reversed (14.7 min) and normal phase HPLC (14.1 min) with authentic 19-OH-AA, (2) derivatization to the corresponding PFB ester, TMS ether derivative yielding a product with a GC retention time (5.7 min) and a NICI−GC−MS fragmentation pattern identical to those of a similarly derivatized synthetic standard of 19-OH-AA with significant major fragment ions at *m*/*z* 391 (100% abundance, loss of PFB), 392, 393 (30 and 26% abundance, reflecting losses of PFB from isotopic [^{13}C]- and [^{14}C]-19-OH-AA, respectively), and 301 (loss of PFB and HOTMS), and (3) catalytic hydrogenation followed by conversion to the corresponding PFB ester, TMS ether derivative yielding a product with a mass spectral fragmentation pattern, under NICI conditions, identical to that of the TMS ether, PFB ester derivative of synthetic 19-hydroxyeicosanoic acid. Fraction B was identified as 20-OH-AA on the basis of the following results: (1) coelution in reversed (15.3 min) and normal phase HPLC (20.5 min) with authentic 20-OH-AA, (2) derivatization to the corresponding PFB ester, TMS ether derivative yielding a product with a GC retention time (5.9 min) and a NICI−GC−MS fragmentation pattern identical to those of a similarly derivatized synthetic standard of 20-OH-AA with significant major fragment ions at *m*/*z* 391 (100% abundance, loss of PFB), 392, 393 (30 and 26% abundance, reflecting losses of PFB from isotopic [^{13}C]- and [^{14}C]-20-OH-AA, respectively), and 301 (loss of PFB and HOTMS), and (3) catalytic hydrogenation followed by conversion to the corresponding PFB ester, TMS ether derivative yielding a product with a mass spectral fragmentation pattern, under NICI conditions, identical to that of the TMS ether, PFB ester derivative of synthetic 20-hydroxyeicosanoic acid. Recently, Wang et al. (*19*), utilizing microsomal fractions isolated from *Sf9* cells expressing CYP 4A2, demonstrated the NADPH-dependent metabolism of AA to 20-OH-AA and 11,12-EET. However, in our studies with purified recombinant CYP 4A2, we were unable to demonstrate significant EET biosynthesis, either in the presence or in the absence of cytochrome b_5 (cytochrome b_5/P450 molar ratios between 0.5 and 2.0) or variable NADPH−cytochrome P450 reductase concentrations (reductase/P450 molar ratios between 1.0 and 20). The reason for these metabolic differences is unknown, but it is interesting that (a) microsomal fractions isolated from CYP 4A2 recombinant baculovirus-infected *Sf9* cells contain additional and yet to be characterized hemoprotein(s), as mentioned above, and (b) microsomal fractions isolated from control, nontransfected *Sf9* insect cells contain an endogenous arachidonic acid epoxygenase activity that generates, in a NADPH-dependent fashion, mixtures of 14,15-, 11,12-, and 8,9-EET, as demonstrated by the radiochromatogram in Figure 6.

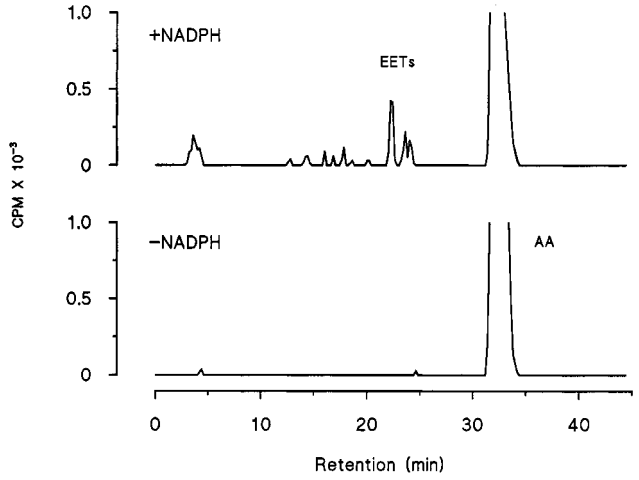

FIGURE 6: Reversed phase HPLC resolution of the metabolites generated by microsomal fractions isolated from control, noninfected *Sf9* insect cells incubated with arachidonic acid. Microsomal fractions isolated from insect cells (1.5 mg/mL) were incubated with [1-^{14}C]AA (75 μM final concentration) and in the presence or absence of NADPH (1 mM final concentration). After 20 min at 35 °C, organic soluble products were extracted into acidified ethyl ether and resolved and quantified as described in Materials and Methods. Shown are the radiochromatograms derived from 20 min incubations containing 0.3 mg of microsomal protein.

As mentioned, under conditions in which we achieved substantial levels of CYP 4A2 expression (70−80 nmol/L of *Sf9* cell culture), we were unable to detect CYP 4A3 biosynthesis by spectral methods. Incubation mixtures containing microsomal fractions isolated from either control or *Sf9* cells infected with CYP 4A3 recombinat viruses catalyzed the NADPH-dependent formation of a product with the reversed phase HPLC properties of EETs. However, control experiments demonstrated that product formation was baculovirus-independent and thus catalyzed by the endogenous insect cell AA epoxygenase activity (Figure 6). From this type of analysis, we concluded that insect cells infected with recombinant CYP 4A3 baculoviruses failed to catalyze the metabolism of AA to a significant extent. To further characterize the expression of CYP 4A3 by enzymatic means, we incubated the insect cell microsomes with [1-^{14}C]LA. In contrast with AA, microsomes from CYP 4A3-transfected cells actively catalyzed LA oxidation to a mixture of 11- and 12-OH-LA (46 ± 2 pmol of product min^{-1} mg of microsomal protein^{-1}, 24 and 76% of the total products, respectively) (Table 2). As with AA, nontransfected insect cells were also capable of catalyzing NADPH-dependent LA oxidation to 12-OH-LA; however, this activity was less than 5% of that observed with CYP 4A3-transfected cells (not shown).

To initiate the characterization of the structural basis for the observed differences between CYP 4A2 and 4A3 in the catalysis of AA oxidation, we generated a cDNA in which the sequence encoding the first 182 amino acids of CYP 4A3 (including the previously discussed A-S-G peptide insertion) was fused to the segment of the CYP 4A2 cDNA encoding the polypeptide that extends from residue 183 to the protein carboxy terminal (Figure 1). This 4A3−4A2 cDNA chimera, as well as the cDNAs encoding CYP2 4A2 and 4A3, was expressed in the baculovirus−insect cell expression system exactly as described in Materials and Methods. Since, as with CYP 4A3, the 4A3−4A2 chimera was also expressed

Table 2: Lauric Acid Hydroxylation by Microsomal Fractions Isolated from Insect Cells Expressing P450 4A cDNA Inserts[a]

		% distribution	
P450 insert	reaction rate (pmol min^{-1} mg of protein^{-1})	11(OH)-LA	12(OH)-LA
4A2	22 ± 2	7	93
4A3	46 ± 2	24	76
4A3−4A2	63 ± 1	25	75

[a] Microsomal fractions (1.5 mg of protein/mL) isolated from *Sf9* insect cells infected with recombinant baculoviruses containing cDNA inserts encoding either CYP 4A2, CYP 4A3, or the CYP 4A3−4A2 chimera were incubated at 35 °C in the presence of a NADPH regenerating system, purified rat liver NADPH−P450 reductase, [1-^{14}C]LA, and NADPH (0.1 μM, 50 μM, and 1 mM final concentrations, respectively). Reactions were terminated by the addition of acidified ethyl ether, and after extraction, the organic soluble products were resolved and quantified as described in the Materials and Methods. Values are averages calculated from four different experiments ± SE.

at levels that could not be detected by spectrophotometric techniques, enzymatic characterizations were carried out using microsomal fractions isolated from insect cells infected with either 4A2, 4A3, or 4A3−4A2 recombinant baculoviruses. When compared to CYP 4A3, insect cell microsomes expressing CYP 4A2 metabolized LA with a substantially higher regioselectivity for the fatty acid ω-carbon atom (93 and 7% of the total products for 12- and 11-OH-LA, respectively, Table 2). On the other hand, the recombinant 4A3−4A2 chimera hydroxylated LA with a regioselectivity nearly identical to that observed with CYP 4A3, forming 11- and 12-OH-LA in a 1/3 molar ratio (Table 2). While microsomal reaction rates are highly dependent on cDNA expression levels, it is interesting that these differences in enzyme regioselectivity were observed using subcellular fractions that metabolized LA at more or less comparable rates (Table 2). Importantly, as with CYP 4A3, the 4A3−4A2 chimera was inactive toward AA. These results suggest that the first 182 residues in CYPs 4A2 and 4A3—including the mentioned CYP 4A2 A-S-G deletion, six conserved substitutions of S for T, K for Q, N for D, T for K, A for T, and D for G, and two nonconserved replacements of P for I and S for F (Figure 1)—provide the protein structural elements that determine the catalysis of AA oxidation and the regioselectivity of LA hydroxylation. As indicated, studies with CYP 2C isoforms (*35*) identified a consensus substrate recognition site within the immediate vicinity of the CYP 4A2 A-S-G deletion. Recent studies with rat CYP 2C11 indicated that a single P for A replacement in the vicinity of the protein amino-terminal domain was sufficient to inhibit heme incorporation during yeast heterologous expression (*37*).

The CYP 4A2 and 4A3 expression experiments summarized above highlighted several important points and considerations. (a) *Sf*9 insect cells possess a microsomal NADPH-dependent monooxygenase. This endogenous enzymatic activity complicates the interpretation of catalytic activities and/or product distribution profiles obtained using microsomal fractions isolated from recombinant baculovirus-transfected cells. (b) Notwithstanding their high sequence homology, under similar conditions, baculovirus-transfected *Sf*9 cells express markedly different levels of spectrally detectable CYPs 4A2 and 4A3. While the molecular reasons for these expression levels remain to be characterized,

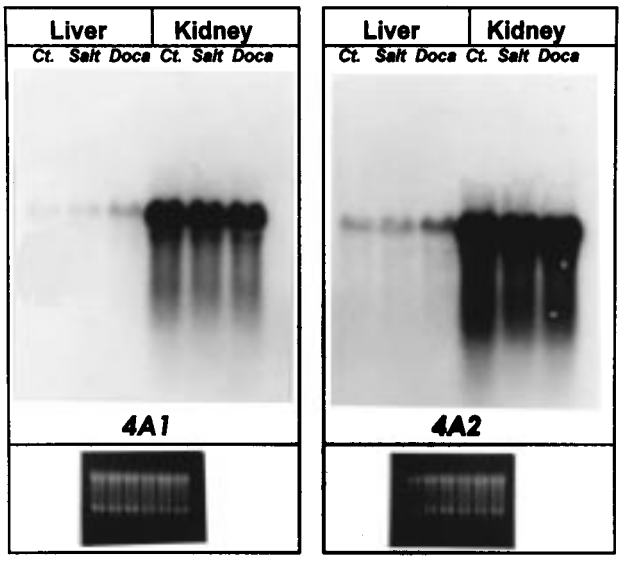

FIGURE 7: Nucleic acid hybridization analysis of RNA samples extracted from control or salt- or DOCA-treated rats. Total RNA samples (20 μg each), isolated from the livers and kidneys of control or high-salt- or DOCA-treated male Sprague-Dawley rats, were submitted to agar electrophoresis, transferred to nitrocellulose membranes, and hybridized to ^{32}P-labeled, gene specific probes described in Materials and Methods and Results and Discussion. After several high-stringency washes, the nitrocellulose membranes were exposed to X-ray films for 12 h. To verify RNA loading and prior to transfer, the agarose−ethidium bromide gels were exposed to UV radiation and photographed. Animal treatment protocols are described in detail in Materials and Methods.

preliminary SDS−PAGE studies indicate the cDNA insert-dependent synthesis of protein(s) with the electrophoretic mobility of CYP 4A3 apoprotein. (c) Despite their high amino acid sequence homologies (Figure 1), CYPs 4A2 and 4A3 behave as catalytically distinct proteins; i.e., while recombinant CYPs 4A2 and 4A3 are active LA hydroxylases, only CYP 4A2 appears to be capable of supporting AA metabolism. (d) With these two highly homologous P450 isoforms, substrate selectivity and product regiochemistry appear to be controlled by structural elements determined by the amino acid sequence of the first 182 residues of the protein.

Organ Expression and Transcriptional Regulation of CYP 4A Genes. The relative tissue distribution and regulation of CYPs 4A1 and 4A2−4A3 were analyzed in RNA samples obtained from the livers and kidneys of control and salt- and DOCA-treated rats. After agar electrophoresis and blotting, membranes were probed with either a 635 or 542 kb fragment containing portions of the untranslated 3′-end of CYP 4A1 or 4A2−4A3, respectively. As shown in Figure 7, CYP 4A1 and 4A2−4A3 transcripts are present at substantially higher levels in the rat kidney than in liver. Animal treatment with DOCA resulted in only minor increases in the concentrations of hepatic mRNAs encoding CYPs 4A1 and 4A2−4A3 (Figure 7) (*22*). On the other hand, excess dietary salt failed to alter the liver or kidney levels of CYP 4A1 or 4A2−4A3 mRNA transcripts (Figure 7). These results are consistent with (a) studies of the regioselective metabolism of AA by rat liver and kidney microsomal fractions demonstrating that while AA ω oxidation, a reaction catalyzed by CYP 4A1, is the predominant metabolic transformation supported by the kidney microsomal enzymes, it accounts for only a minor portion of the AA metabolites generated by liver microsomes (*2*, *3*, *12*, *38*); (b) the reported effects of DOCA treatment on the AA monooxygenase activities of rabbit kidney microsomal fractions (*22*); and (c) published data indicating that excess dietary salt resulted in an increased kidney AA epoxygenase activity but it had no significant effects on the renal ω and $\omega - 1$ monooxygenases (*12*). As mentioned, published hybridization data showed that while CYPs 4A1 and 4A3 were expressed preferentially in rat liver, CYPs 4A2 and 4A8 predominated in the kidney (*14*, *15*, *25*−*27*, *33*, *34*).

The sex specific expression of P450 isoforms in the rat has been demonstrated (*34*, *39*, and references therein). Among these, CYPs 2C11, 3A2, and 4A2 are considered male specific and CYP 2C12 is considered female specific (*34*, *39*). Because the high degree of sequence homology between CYPs 4A2 and 4A3, even in the areas recognized by the sequence specific probes utilized in those experiments (*34*), complicates the interpretation of observed differences in their sex and tissue specific expression, we developed a methodology for their further characterization. The presence in the CYP 4A3 cDNA of the nine extra and 121 bp nucleotide segments (Figures 1 and 2) afforded the means for unequivocal characterization. Two different but complementary approaches were utilized for these studies: (a) nucleic acid hybridization blot analysis with either a 4A3 probe encoding the CYP 4A3 specific 121 bp segment (between nucleotides 1552 and 1674, from the ATG initiation codon), a CYP 4A2 specific 123 bp probe encoding the first 62 and 61 nucleotides upstream and downstream of the 123 intron separating exons 12 and 13, respectively (Figure 2), or the CYP 4A1 specific probe utilized above; and (b) RT-PCR amplification of total RNA using P450 isoform specific PCR primers. The results of the hybridization studies are shown in Figure 8A. To document the specificity of these probes, control experiments were performed using the CYP 4A2 and 4A3 cDNAs. As shown in Figure 8B, the CYP 4A3 probe was selective for its cDNA. On the other hand, while the 4A2 probe hybridized preferentially with its cDNA, it also interacted, to a modest extent, with the 4A3 cDNA. The hybridization data shown in Figure 8A support the following conclusions. (a) With the exclusion of CYP 4A2 in the female liver, all three 4A isoforms are expressed in the male and female liver and kidney. (b) CYPs 4A1, 4A2, and 4A3 are expressed at substantially higher levels in kidney than in liver. (c) In male kidney, the predominant 4A isoform is CYP 4A2 followed by 4A3 and substantially lower levels of CYP 4A1. (d) In the female kidney, the mRNAs encoding all three isoforms are present at more or less comparable levels. These results were corroborated by the RT-PCR approach outlined above. Thus, the data in Figure 8C confirmed (a) the cDNA isoform selectivity of the PCR amplification primers (Figure 8, lanes 9−12), (b) that CYPs 4A2 and 4A3 predominate in the male and female kidneys (Figure 8C, lanes 1−8), (c) that CYP 4A2, expressed at nearly undetectable levels in the female liver (*34*, *39*) (Figure 8C, lane 7), is expressed at significant levels in the female kidney (Figure 8C, lane 4), and (d) that while the female liver contains significant levels of CYP 4A3 transcripts (Figure 8C, lane 8), these are nearly undetectable in the male liver (Figure 8C, lane 6). The data in this figure also illustrate a described size difference between the 4A2 and

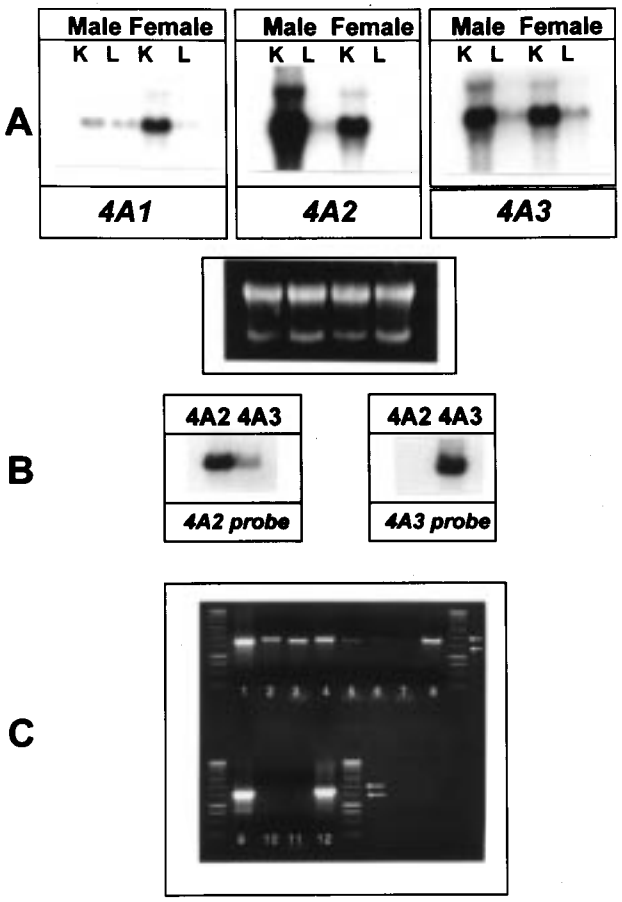

FIGURE 8: Sex and organ specificity in the expression of CYP 4A1, 4A2, and 4A3 mRNA transcripts. Samples of total RNA isolated from the livers (L) and the kidneys (K) of male and female Sprague-Dawley rats were either submitted to agar electrophoresis (20 μg each) or utilized as templates for RT-PCR (5 μg each). (A, Northern blots) Electrophoresed RNAs were transferred to nitrocellulose membranes and exposed to the ^{32}P-labeled, gene specific probes described in Materials and Methods or Results and Discussion. After high-stringency washes, the membranes were exposed to X-ray films for 12−24 h. To verify RNA loading and prior to transfer, the agarose−ethidium bromide gels were exposed to UV radiation and photographed. (B, Southern blots) Samples of the cDNAs encoding CYPs 4A2 and 4A3 (2 μg each) were submitted to agar gel electrophoresis, transferred to nitrocellulose membranes, and probed with the above 4A2 or 4A3 gene specific probes. After high-stringency washes, the membranes were exposed to X-ray film for 4−6 h. (C, PCR) Aliquots of the total RNA samples described above (5 μg each) were utilized as templates for oligo-(dT)-primed, reverse transcriptase (RT)-catalyzed DNA generation. Approximately 5% of the RT products were then utilized as templates for PCR amplification of the CYP 4A2 (1647 bp, lane 9) and 4A3 (1762 bp, lane 12) specific fragments described in Results and Discussion. PCR products were loaded as follows: lanes 1 and 2, male kidney; lanes 3 and 4, female kidney; lanes 5 and 6, male liver; lanes 7 and 8, female liver; lanes 9 and 10, CYP 4A2 cDNA; and lanes 11 and 12, CYP 4A3 cDNA. CYP 4A2 (odd-numbered lanes) and 4A3 (even-numbered lanes) specific primers were utilized for PCR amplification.

4A3 PCR products resulting from the differential processing of the 123 bp intron that is spliced for CYP 4A2 and preserved in the 4A3 mRNA (Figures 2 and 8C).

An unexpected result was the absence of detectable anti-4A2 immunoreactive protein(s) in microsomal fractions isolated from male liver and the nearly undetectable levels of the CYP 4A2 protein in female kidney microsomes (Figure 9). In the presence of measurable levels of mRNA transcripts

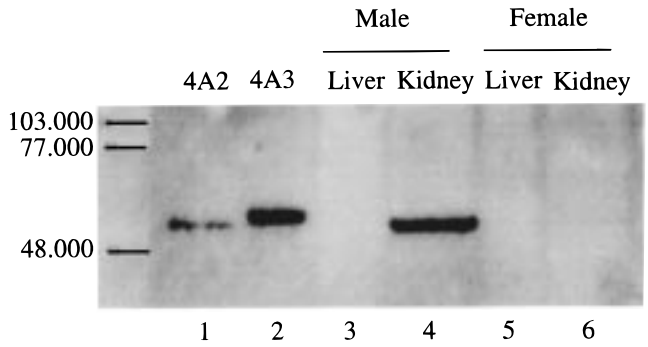

FIGURE 9: Immunoelectrophoresis of liver and kidney microsomal fractions isolated from male and female rats. Microsomal fractions (25 μg each), isolated from the livers and kidneys of male and female rats, were submitted to discontinuous SDS−PAGE as described in Materials and Methods. After electrophoretic transfer, the PVDF membranes were incubated with a solution of affinity-purified anti-cytochrome P450 4A2 (2 μg/mL). Immunoreactive proteins were visualized by the use of a horseradish peroxidase-coupled anti-rabbit IgG and a SuperSignal Substrate Western Blotting kit (Pierce). Sample loading was as follows: lanes 1 and 2, cell lysates obtained from *Sf9* cells infected with recombinant CYP 4A2 and 4A3 baculoviruses, respectively; lanes 3 and 4, male liver and kidney microsomes, respectively; and lanes 5 and 6, female liver and kidney microsomes, respectively. The relative electrophoretic mobility of selected protein molecular weight standards is indicated.

encoding CYP 4A2 in the male liver and in the male and female kidneys, only with male kidney microsomal fractions did we observe the presence of significant anti-4A2 immunoreactive material (Figure 9). On the other hand, high protein loadings and long exposures yielded a weak protein band, indicative of low levels of the CYP 4A2 protein in the female rat kidney. These results suggest either gender and organ specific translational control of CYP 4A2 biosynthesis or, alternatively, a high rate of turnover for female CYP 4A2. As shown in Figure 9, the anti-CYP 4A2 antibody was also immunoreactive toward recombinant CYP 4A3. However, recombinant CYP 4A2 could be distinguished from CYP 4A3 by its size difference (Figure 9). The data in Figure 9 also indicate that the levels of CYP 4A3 protein in rat liver and kidney microsomes are nearly undetectable. Other than the three amino acid deletions mentioned in CYP 4A2, CYPs 4A2 and 4A3 share extensive amino acid sequence homology, including complete identity in the 70 amino acids that flank both sides of the heme binding cysteine (Figure 1). As indicated above, heme incorporation into the full length CYP 4A3 polypeptide synthesized by CYP 4A3- and recombinant baculovirus-infected *Sf9* insect cells appears to be impaired (Figures 3 and 9). It is possible that the biosynthesis of a nonfunctional CYP 4A3 polypeptide in rat liver and kidney signals its rapid degradation and turnover. Regardless of the causative mechanism(s), our data show that CYP 4A3 gene transcription does not result in immunodetectable levels of CYP 4A3 protein.

Regulation of CYPs 4A2 and 4A1 during Salt Sensitive Experimental Hypertension. A role for the renal P450-dependent AA ω and $\omega - 1$ oxygenase in the control of systemic blood pressure was initially proposed by McGiff and collaborators in 1988 (*7*, *9*). In those initial studies, changes in the activities of the renal AA ω and $\omega - 1$ oxygenase were temporally associated with the onset of

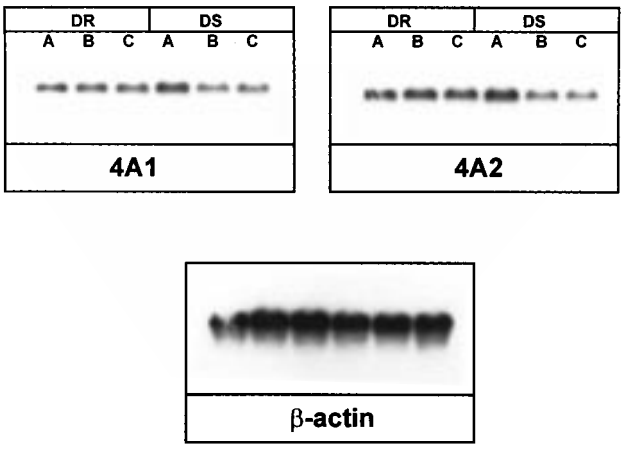

FIGURE 10: Nucleic acid hybridization analysis of RNA samples obtained from control or salt-treated Dahl salt resistant and salt sensitive rats. Total RNA samples (20 μg each), isolated from the kidneys of Dahl salt resistant (DR) or salt sensitive (DS) rats fed either a control (0.3% NaCl) (A) or a high-salt diet (8% NaCl) for a total of 15 (C) or 18 (B) days, were submitted to agar electrophoresis, transferred to nitrocellulose membranes, and hybridized to ^{32}P-labeled, gene specific probes as described in Material and Methods. After several high-stringency washes, the nitrocellulose membranes were exposed to X-ray films for 12 h.

hypertension in the SHR/WKY rat model of spontaneous hypertension (*7*, *9*). Studies with the SHR rat demonstrated the preferential expression of the 4A2 gene in hypertensive SHR rats (*20*), and the age-dependent transcriptional upregulation of kidney mRNAs recognized by a 4A1 cDNA probe (*7*, *9*). An integration of metabolic and biological activity data has led to the proposal of a prohypertensive role for the products of the kidney AA ω and $\omega - 1$ oxygenase (*8*, *9*). More recently, functional and genetic data have extended this prohypertensive role to include salt sensitivity in the Dahl rat model of salt sensitive hypertension (*11*). The salt-dependent transcriptional regulation of the CYP 4A1 and 4A2 genes and its relationship to the development of salt sensitive hypertension were studied in Dahl salt sensitive and salt resistant rats fed low- and high-salt diets for 14−18 days (*10*). Groups of hypertensive Dahl salt sensitive rats (MABP $\leq$ 185−200 mmHg) and of normotensive high- and low-salt-treated Dahl salt resistant and low-salt-treated Dahl salt sensitive rats (MABP $\leq$ 135 mmHg) were sacrificed, and the total kidney RNA was isolated and submitted to Northern blot analysis using the gene specific probes described in Materials and Methods. As shown in Figure 10, no significant differences were observed between normotensive Dahl salt resistant and hypertensive Dahl salt sensitive rats in the concentrations and/or salt regulation of their kidney CYP 4A1 and 4A2 isoforms. Furthermore, immunoelectrophoresis of microsomal fractions isolated from the kidneys of these animals also failed to show differences in the levels of anti-CYP 4A1 or 4A2 immunoreactive material between these animals (not shown). These results are interesting in that studies with the SHR rat model of spontaneous hypertension have shown an association between the development of high blood pressure, the upregulation of the 4A2 gene, and the biosynthesis of prohypertensive arachidonic acid ω and $\omega - 1$ alcohols (*7*, *9*, *20*). Thus, it would appear that products of the AA ω and $\omega - 1$ monooxygenase play different roles in the pathophysiology of experimental spontaneous and salt sensitive hypertension. Finally, the expression of CYPs 4A2 and 4A3 in the kidneys of both DR and DS animals was confirmed by RT-PCR analysis of total kidney RNAs using the 4A2 and 4A3 specific PCR primers described above (data not shown).

Studies by Sundseth and Waxman (*34*) demonstrated the male specific expression of CYP 4A2 in liver and kidney. Furthermore, continuos exposure to plasma growth hormone, a hormone profile characteristic of female rats, fully suppressed male liver but not male kidney CYP 4A2 expression and suggested organ specific hormonal control of sexual dimorphic CYP 4A2 expression (*34*). Our studies, showing liver but not kidney male specific expression of CYP 4A2, document an organ specific sexual dimorphism in CYP 4A2 expression. Furthermore, these results raise interesting questions with regard to the commonality of growth hormone and/or androgen-dependent mechanisms for the control of P450 gene expression and transcription, particularly in extrahepatic tissues (*34*). In light of the reported lower susceptibility of female rats to clofibrate-induced peroxisome proliferation, it would be interesting to re-examine the role that these inducers play in the regulation of male and female kidney CYPs 4A2 and 4A3 (*34*, *40*). Recent studies of the metabolism of lauric acid by murine microsomal fractions suggest strain- and sex-dependent differences in the constitutive expression of mouse hepatic CYP 4A isoforms (*41*).

An unresolved issue is that of the differential processing of the highly homologous CYP 4A2 and 4A3 gene transcripts. As discussed and illustrated in Figure 2, a 123 bp segment expressed as part of exon 12 in the CYP 4A3 mRNA is recognized as an intronic sequence, spliced, and removed from the final 450 4A2 mRNA product. However, canonical splice acceptor−donor sequences are present at both intron−exon boundaries for the spliced (4A2) and nonspliced (4A3) genes (Figure 2). Furthermore, the nucleotide sequences immediately upstream or downstream of this gene specific splice region are also highly conserved (Figure 2) (*26*, *27*). Additionally, the PCR amplification data presented in Figure 8 demonstrate that only the spliced or the nonspliced transcripts are generated from the 4A2 or the 4A3 genes, respectively. The molecular basis for this gene specific differential splice mechanism for these two, otherwise highly homologous, genes remains to be determined.

In summary, we report here the molecular and enzymatic characterization of CYP 4A2, a P450 isoform implicated in the biosynthesis of prohypertensive AA metabolites. Additionally, we characterize CYP 4A2 as the predominant 4A isoform expressed in male and female kidneys and demonstrate an organ specific sexual dimorphism in the control of CYP 4A2 mRNA levels. Our results also show that, despite high levels of mRNA transcripts, the concentrations of translated CYPs 4A2 and 4A3 polypeptides can be either limited (4A2) or undetectable (4A3). Finally, as a participant in the oxidative metabolism of AA to 19- and 20-OH-AA, CYP 4A2 may play central roles in the biosynthesis of biologically active eicosanoids and, therefore, may have important roles in kidney physiology. The structural, spectral, and enzymatic characterization described here should facilitate future studies of the significance of these P450 isoforms in the in vivo bioactivation of endogenous AA pools.

REFERENCES

1. Capdevila, J. H., Chacos, N., Werringloer, J., Prough, R. A., and Estabrook, R. W. (1981) *Proc. Natl. Acad. Sci. U.S.A. 78*, 5362−5366.
2. Oliw, E. H., and Oates, J. A. (1981) *Biochim. Biophys. Acta 666*, 327−340.
3. Morrison, A. R., and Pascoe, N. (1981) *Proc. Natl. Acad. Sci. U.S.A. 78*, 7375−7378.
4. Capdevila, J. H., Zeldin, D., Makita, K., Karara, A., and Falck, J. R. (1995) in *Cytochrome P450: Structure, Mechanism, and Biochemistry* (Ortiz de Montellano, P., Ed.) 2nd ed., pp 443−471, Plenum Press, New York.
5. Makita, K., Falck, J. R., and Capdevila, J. H. (1996) *FASEB J. 10*, 1456−1463.
6. Oliw, E. H., Bylund, J., and Herman, C. (1996) *Lipids 31*, 1003−1021.
7. McGiff, J. C. (1991) *Annu. Rev. Pharmacol. Toxicol. 31*, 339−369.
8. Harder, D. R., Campbell, W. B., and Roman, R. J. (1995) *J. Vasc. Res. 32*, 79−92.
9. MacGiff, J. C., Steinberg, M., and Quilley, J. (1996) *Trends Cardiovasc. Med. 6*, 4−10.
10. Makita, K., Takahashi, K., Karara, A., Jacobson, H. R., Falck, J. R., and Capdevila, J. H. (1994) *J. Clin. Invest. 94*, 2414−2420.
11. Stec, D. E., Deng, A. Y., Rapp, J. P., and Roman, R. J. (1996) *Hypertension 27*, 564−568.
12. Capdevila, J. H., Wei, S., Yan, Y., Karara, A., Jacobson, H. R., Falck, J. R., Guengerich, F. P., and DuBois, R. N. (1992) *J. Biol. Chem. 267*, 21720−21726.
13. Karara, A., Makita, K., Jacobson, J. R., Falck, J. R., Guengerich, F. P., DuBois, R. N., and Capdevila, J. H. (1993) *J. Biol. Chem. 268*, 13565−13570.
14. Gonzalez, F. J. (1989) *Pharmacol. Rev. 40*, 243−288.
15. Okita, R. T. (1994) in *Peroxisome Proliferators: Unique Inducers of Drug-Metabolizing Enzymes* (Moody, D. E., Ed.) pp 37−49, CRC Press, Boca Raton, FL.
16. Nelson, D. R., Kamataki, T., Waxman, D. J., Guengerich, F. P., Estabrook, R. W., Feyereisen, R., Gonzalez, F. J., Coon, M. J., Gunsalus, I. C., Gotoh, O., Okuda, K., and Nebert, D. W. (1993) The P450 superfamily: Update on new sequences, gene mapping, accession numbers, early trivial names of enzymes and nomenclature, *DNA Cell Biol. 12*, 1−51.
17. Bains, S. K., Gardiner, S. M., Manniveiler, K., Gillett, D., and Gibson, G. C. (1985) *Biochem. Pharmacol. 34*, 3221−3229.
18. Imaoka, S., Tanaka, S., and Funae, Y. (1989) *Biochem. Int. 18*, 731−740.
19. Wang, M.-H., Stec, D. E., Balazy, M., Mastyugin, V., Yang, C. S., Roman, R. J., and Schwartzman, M. L. (1997) *Arch. Biochem. Biophys. 336*, 240−250.
20. Iwai, N., and Inagami, T. (1991) *Hypertension 17*, 161−169.
21. Stec, D. E., Trolliet, M. R., Krieger, J. E., Jacob, H. J., and Roman, R. J. (1996) *Hypertension 27*, 1329−1336.
22. Lapuerta, L., Chacos, N., Falck, J. R., Jacobson, H., and Capdevila, J. H. (1998) *Am. J. Med. Sci. 31*, 275−279.
23. Sanger, F., Nicklen, S., and Coulson, A. R. (1977) *Proc. Natl. Acad. Sci. U.S.A. 74*, 5463−5467.
24. McDonald, R. J., Swift, G. H., Przybyla, A. E., and Chirgwin, J. M. (1987) *Methods Enzymol. 152*, 219−235.
25. Hardwick, J. P., Song, B. J., Huberman, E., and Gonzalez, F. J. (1987) *J. Biol. Chem. 262*, 801−810.
26. Kimura, S., Hanioka, N., Matsunaga, E., and Gonzalez, F. J. (1989) *DNA 8*, 503−516.
27. Kimura, S., Hardwick, J. P., Kozak, C. A., and Gonzalez, F. J. (1989) *DNA 8*, 517−525.
28. Zeldin, D. C., DuBois, R. N., Falck, J. R., and Capdevila, J. H. (1995) *Arch. Biochem. Biophys. 322*, 76−86.
29. Capdevila, J. H., Falck, J. R., Dishman, E., and Karara, A. (1990) *Methods Enzymol. 187*, 385−394.
30. Capdevila, J. H., Dishman, E., Karara, A., and Falck, J. R. (1991) *Methods Enzymol. 206*, 441−453.
31. Omura, T., and Sato, R. (1964) *J. Biol. Chem. 239*, 2370−2378.
32. Matsudaira, P. (1987) *J. Biol. Chem. 262*, 10035−10038.
33. Stromstedt, M., Hayashi, S., Zaphiropoulos, P. G., and Gusftafsson, J. A. (1990) *DNA Cell Biol. 9*, 569−577.
34. Sundseth, S. S., and Waxman, D. J. (1992) *J. Biol. Chem. 267*, 3915−3921.
35. Gotoh, O. (1992) *J. Biol. Chem. 267*, 83−90.
36. Gonzalez, F. J., Kimura, S., Tamura, S., and Gelboin, H. V. (1991) *Methods Enzymol. 206*, 93−99.
37. Yamazaki, S., Sato, K., Suhara, K., Sakaguchi, M., Mihara, K., and Omura, T. (1993) *J. Biochem. 114*, 652−657.
38. Capdevila, J. H., Kim, Y. R., Martin-Wixtrom, C., Falck, J. R., Manna, S., and Estabrook, R. W. (1985) *Arch. Biochem. Biophys. 243*, 8−19.
39. Lund, J., Zaphiropoulos, P. G., Mode, A., Warner, M., and Gustafsson, J. A. (1991) *Adv. Pharmacol. 22*, 325−354.
40. Johnson, E. F., Palmer, C. N. A., Griffin, K. J., and Mei-Hui, H. (1996) *FASEB J. 10*, 1241−1248.
41. Hiratsuka, M., Matsuura, T., Watanabe, E., Sato, M., and Suzuki, Y. (1996) *J. Biochem. 119*, 340−345.

BI981048G